

# Comparison of Radiation Hardness of P-in-N, N-in-N, and N-in-P Silicon Pad Detectors

M. Lozano, G. Pellegrini, C. Fleta, C. Loderer, J. M. Rafí, M. Ullán, F. Campabadal, C. Martínez, M. Key, G. Casse, and P. Allport

**Abstract**—The very high radiation fluence expected at LHC (Large Hadron Collider) at CERN will induce serious changes in the electrical properties of the silicon detectors that will be used in the internal layers of the experiments (ATLAS, CMS, LHCb). To understand the influence of the fabrication technology in the radiation-induced degradation, silicon detectors were fabricated simultaneously with the three different possible technologies, P-in-N, N-in-N, and N-in-P, on standard and oxygenated float-zone silicon wafers. The diodes were irradiated with protons to fluences up to  $10^{15}$  cm<sup>-2</sup>. The measurements of the electrical characteristics, current-voltage and capacitance-voltage, are presented for the detectors manufactured with the three technologies. In terms of alpha factor (leakage current) the three technologies behave similarly. In terms of beta factor (effective doping concentration) N-in-P devices show the best performances.

**Index Terms**—Detector technology, N-in-N, N-in-P, P-in-N, radiation hardness, silicon radiation detectors.

## I. INTRODUCTION

THE study and quest for new radiation hard silicon detectors has become very active in recent years. Because of their high efficiency, small thickness and fast readout, silicon detectors are widely used in high energy physics experiments, including future experiments such as those at the Large Hadron Collider (LHC). The LHC will bring proton beams into collision at centre of mass energies up to 14 TeV. The very high luminosity foreseen ( $\sim 10^{34}$  cm<sup>-2</sup>s<sup>-1</sup>) implies that the ATLAS Semiconductor Tracker will be exposed to fluences up to  $1.4 \times 10^{14}$  cm<sup>-2</sup> 1-MeV(Si) neutron equivalent over the ten years of operation [1].

Under these conditions, detector performance may be limited by a large number of defects introduced into the device. The bulk displacement damage results in a change of the dopant concentration due to the introduction of deep levels. N-type detectors (standard P-in-N) become progressively less n-type with the increasing of the hadron fluence until they invert to effectively p-type at around  $2 \times 10^{13}$  cm<sup>-2</sup> 1-MeV(Si) neutron equivalent and then continue to become more p-type beyond this

Manuscript received January 11, 2005; revised March 31, 2005. This work was supported in part by the Spanish CICYT project FPA2003-03878-C02-02 and was performed in the framework of CERN RD50 project.

M. Lozano, G. Pellegrini, C. Fleta, J. M. Rafí, M. Ullán, F. Campabadal, C. Martínez, and M. Key are with the Centro Nacional de Microelectrónica, IMB-CNM (CSIC), Barcelona, 08193, Spain (e-mail: manuel.lozano@cnm.es).

C. Loderer is with the IMB-CNM and the University of Applied Science, Munich 80335, Germany.

G. Casse and P. Allport are with the Oliver Lodge Laboratory, The University of Liverpool, Liverpool, U.K.

Digital Object Identifier 10.1109/TNS.2005.855809

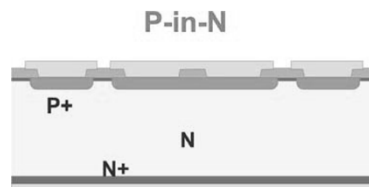


Fig. 1. Cross section of a P-in-N detector.

point. However, the detector still works beyond the inversion point because the junction moves from the P<sup>+</sup> contact to the N<sup>+</sup> back-plane contact.

The multiple advantages of using N-in-N or N-in-P configurations come out when they are used as microstrip or pixel detectors. The advantage of N-in-N detectors exposed to high radiation fluences environment is that the bulk silicon depletes from the strip side following type inversion, and therefore signal collection is assured even if the bulk is only partially depleted [2], [3]. Instead, in N-in-P detectors, type inversion is not foreseen, but only a constant increasing of the concentration of the p-type bulk [4].

In this paper we present for the first time a direct comparison of the radiation hardness of detectors manufactured simultaneously in the three different technologies irradiated with 24 GeV protons up to fluences of  $10^{15}$  cm<sup>-2</sup>.

## II. TECHNOLOGY

There are three possible technologies to fabricate silicon micro-strip radiation detectors: P-in-N, N-in-P, and N-in-N. Each one has advantages and drawbacks.

### A. P-in-N Technology

Fig. 1 shows an example of the P-in-N technology. This is the most used configuration for radiation detectors in the form of microstrip and pixel detectors. The technology is simpler, the detector only needs six mask levels, and therefore, they are cheaper when compared to other technologies. By using oxygenated silicon, they can withstand radiation fluences higher than  $3 \times 10^{14}$  protons/cm<sup>2</sup>, which represents the fluence achieved in the ATLAS experiment at CERN in ten years of operation [1]. Nevertheless, if the LHC is upgraded to higher luminosities, as it is foreseen, the radiation dose to be supported by the detectors will be one order of magnitude higher, and this P-in-N technology will not be adequate. For this reason, it has been proposed to replace these type of detectors in the future, and not use them in experiments with higher radiation doses.

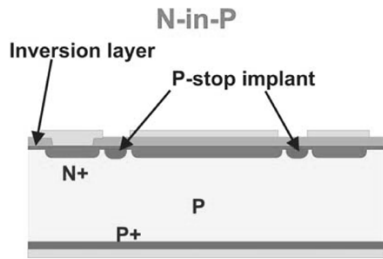


Fig. 2. Cross section of a N-in-P detector with p-stop implants.

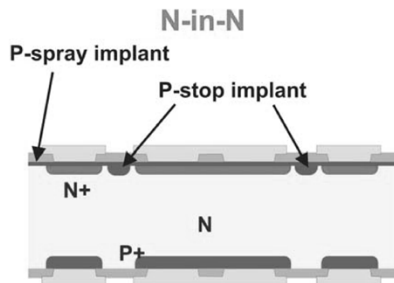


Fig. 3. Cross section of a N-in-N detector with p-spray and p-stop implants, and back side processing.

### B. N-in-P Technology

Although this technology has been less studied in past years, N-in-P detectors are expected to be more radiation hard than standard P-in-N detectors. This is due to the fact that the bulk is already P type and therefore no type inversion is expected.

These detectors are more complex as they need an extra surface insulation. This insulation is achieved either by a blank surface implant, named P-spray, or by P-type junctions, named P-stops. This technology requires seven mask levels. A schematic cross section of this type of technology with p-stop implantation is shown in Fig. 2. These detectors have been fabricated with implanted p-stops with a dose of  $10^{13}$  and  $10^{14}$   $\text{cm}^{-2}$  in oxygenated and standard P-type silicon substrates.

### C. N-in-N Technology

Finally, N-in-N detectors are expected to withstand up to  $10^{15}$  protons/ $\text{cm}^2$  [5] and Fig. 3 shows a schematic cross section of this type of technology. They require ten mask levels and need double side processing, making the technology the most complex of the three. Our detectors have been fabricated with implanted p-stops doses of  $10^{13}$  and  $10^{14}$   $\text{cm}^{-2}$  in standard N-type silicon substrates and with a implanted p-stop dose of  $10^{13}$   $\text{cm}^{-2}$  in oxygenated N-type silicon substrates.

For simplicity, in the detectors used in this study, there is no backside processing, only blank backside implant and metallization was performed. Also no p-spray was implanted.

### D. Fabrication Information

All the detectors have been fabricated in standard and oxygenated substrates, 280  $\mu\text{m}$  thick, using a mask set designed by Liverpool University and IMB-CNM which includes microstrip and pad detectors of different geometries. In this work we

used pad diodes with a sensitive area of  $5 \times 5 \text{ mm}^2$ . The bulk resistivity of both types of wafers was  $4 \text{ k}\Omega \cdot \text{cm}$ . This corresponds to a concentration of  $3.3 \times 10^{12} \text{ cm}^{-3}$  for boron dopants and  $1.0 \times 10^{12} \text{ cm}^{-3}$  for phosphorus dopants, for P- and N-type substrates respectively.

The detectors have a guard ring 200  $\mu\text{m}$  wide and a hole in the metalization for light injection if needed. The separation between the guard ring and the sensitive area is 100  $\mu\text{m}$ . The junctions were formed by implantation of boron (P-type) or phosphorus (N-type) whereas the metalization (1  $\mu\text{m}$  for all contacts) was deposited by aluminum sputtering. In order to optimize the breakdown voltage, in N-in-P and N-in-N technologies, different values of P-stop implant doses have been evaluated.

The samples were fabricated along with full microstrip detectors in the same mask set. Therefore, although these are pad detectors, the thermal budget is the same as for complete ac-coupled microstrip detectors with polysilicon bias resistors.

The oxygenations were carried out in quartz tubes and in wet ( $\text{H}_2 + \text{O}_2$ ) environment at a temperature of 1150  $^\circ\text{C}$ . The processing consisted of an initial oxidation of 12 h, followed by a diffusion step in  $\text{N}_2$  ambient for 48 h. No trichloroethane (TCA) was added since it has been shown that this deteriorates the characteristics of the diodes [6].

### E. Radiation and Anneal Information

The detectors were irradiated at different fluences with a 24 GeV proton beam at the CERN PS facilities, at room temperature and without bias. The fluences were  $7.73 \times 10^{12}$ ,  $7.87 \times 10^{13}$ ,  $3.84 \times 10^{14}$ , and  $1.02 \times 10^{15}$  protons per square cm for N-in-P and P-in-N technologies; for N-in-N, the irradiation at the smallest fluence,  $7.73 \times 10^{12}$ , was not performed.

The proton fluences were determined by the Radiation-Test Facility at CERN [7] by activation measurements of aluminum foils placed at the back of the detectors. The fluences reported can be normalized to 1-MeV(Si) neutron equivalent fluence by the NIEL factor  $0.62 \text{ keVcm}^2/\text{g}$  [8].

After each irradiation step the diodes were subjected to a short term annealing of 4 min at 80  $^\circ\text{C}$  previous to the measurements to ensure that all were measured at the same annealing stage. At this stage the change in the effective doping concentration reaches a flat minimum [9].

In addition, this annealing stage corresponds to approximately two weeks at room temperature, which is the expected maintenance period at ATLAS experiments.

## III. ELECTRICAL CHARACTERISTICS

A shielded probe station, Karl Suss PA200, was used for electrical probing. The sample and contacting probes were placed in a Faraday cage to provide an electrical shielding and keep them dark. The diodes were connected to the measuring electronics by two probe needles, one was connected to the central pad and the other one to the guard ring. The chuck was used to connect the back contact of the diode to ground. Two Keithley 2410 Source Meters were used to apply voltages and measure the two different currents separately. One of the SourceMeters was used to apply the high voltage to the guard ring while the

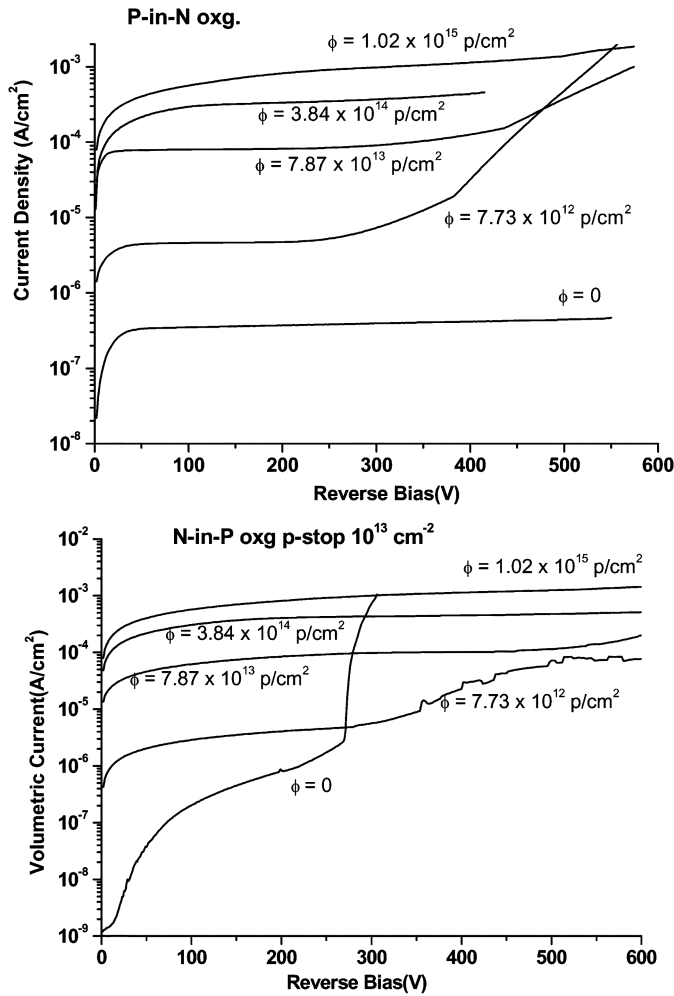


Fig. 4. Leakage current densities of P-in-N (top) and N-in-P (bottom) detectors at different fluences.

other one was used to apply the same voltage to the pad. In this way the surface current was collected by the guard ring.

The capacitance was measured with an Impedance Analyzer HP 4192A operated at 10 kHz. Additionally, a bench was used to measure the capacitance (CV) at high voltage, up to 1100 V. In this configuration, leakage currents of both central pad and guard ring were measured simultaneously.

All measurements had been carried out at a temperature between 19 °C and 22 °C and then normalized to 20 °C. After irradiation, the detectors were stored at -35 °C.

#### A. Leakage Current

The leakage currents density versus reverse bias of non irradiated and irradiated P-in-N and N-in-P detectors at different proton fluences, up to  $10^{15}$  p/cm<sup>2</sup>, are shown in Fig. 4.

The values obtained for the leakage current for P-in-N detectors are very low, in agreement with previous results from other batches, and well below the maximum tolerable values accepted by the ATLAS experiment.

Non irradiated N-in-P detectors have a leakage current of 200 nA/cm<sup>2</sup> at 100 V range, and a breakdown voltage of 300 V. It must be noticed that these type of detectors do not reach full depletion before junction breakdown. This is due to the electric

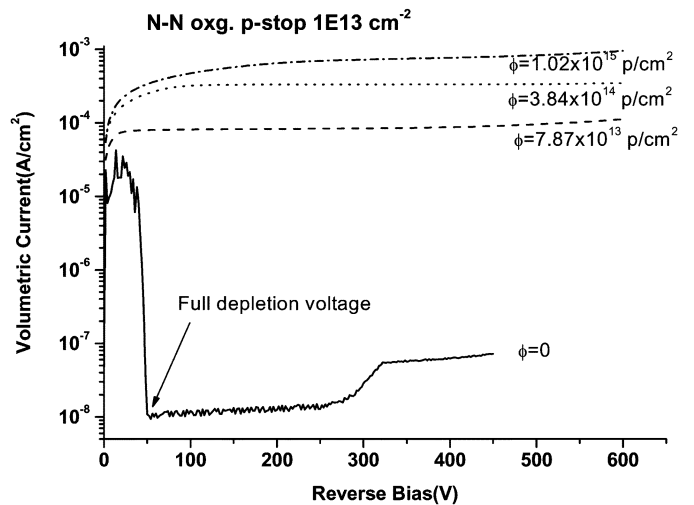


Fig. 5. Leakage current densities for N-in-N detectors, with p-stop implants of  $10^{13}$  cm<sup>-2</sup> and irradiated at different fluences.

field of the N-P junction which cannot expand beyond the p-stop implantation. The p-stop is used to insulate the diode from the guard ring, but has the effect of lowering the breakdown voltage as it behaves as a virtual ground. After irradiation full depletion can be reached and values of leakage current density are similar to the obtained for standard P-in-N detectors.

Non irradiated N-in-N detectors have a very high side surface current, on the order of mA, due to the damage in the silicon lattice. This damage is localized onto the device sides where the chips are cut. However, when the guard ring reaches full depletion, insulating the active junction from the chips sides, the current density decreases to values smaller than 10 nA/cm<sup>2</sup>. Fig. 5 shows the characteristic of the leakage current across the central pad at different proton fluences. It must be noticed that even if these N-in-N detectors did not have backside processing, after full depletion the leakage current density becomes smaller than that of the standard P-in-N detectors fabricated on the same substrate.

None of the irradiated N-in-N diodes showed the high guard ring current density. This is due to the substrate inversion from N-type to P-type, in which the junction moves from the bottom to the top side, and the junction short at the bottom disappears.

Detectors fabricated with the three technologies and irradiated with a proton fluence of  $10^{15}$  p/cm<sup>2</sup> present similar leakage currents in the range of mA/cm<sup>2</sup>. The breakdown voltage of non irradiated N-in-N and N-in-P detectors was measured to be 300 V while for non irradiated P-in-N detectors it was higher than 600 V. These values of breakdown voltages are much higher than the full depletion voltages,  $V_{FD}$ , which are in the range from 50 to 80 V for P-in-N, and N-in-N technologies. Unfortunately, this condition is not achieved in the nonirradiated N-in-P detectors, and therefore their values of  $V_{FD}$  do not appear in the Table I.

#### B. Capacitance-Voltage

Capacitance-voltage characteristics were used to calculate the full depletion voltage of the detectors under study. The standard procedure used for the extraction of  $V_{FD}$  was a crossing of two

TABLE I  
 FULL DEPLETION VOLTAGE OF P-IN-N AND N-IN-P DETECTORS

Technology	P in N		N in P	
	Std	Oxg	Std	Oxg
P-stop	-	-	$10^{13} \text{ cm}^{-2}$	
Substrate	Std	Oxg	Std	Oxg
Non irradiated (V)	$78 \pm 7$	$63 \pm 6$	----	----
Irrad. fluence $10^{15} \text{ protons/cm}^2$ (V)	$479 \pm 47$	$423 \pm 40$	$503 \pm 49$	$433 \pm 44$

 TABLE II  
 FULL DEPLETION VOLTAGE OF N-IN-N DETECTORS

Technology	N in N		
	$10^{14} \text{ cm}^{-2}$	$10^{13} \text{ cm}^{-2}$	
P-stop		Std	Oxg
Substrate	Std	Std	Oxg
Non irradiated (V)	$49 \pm 5$	$58 \pm 5$	$54 \pm 5$
Irrad. fluence $10^{15} \text{ protons/cm}^2$ (V)	$391 \pm 37$	$320 \pm 31$	$444 \pm 41$

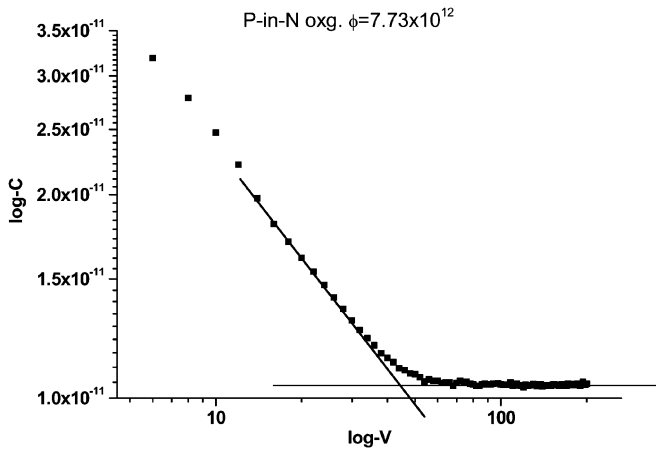


Fig. 6. Example of the log-C versus log-V plot used to calculate the full depletion voltage.

straight lines in the logC-logV plot near the kink. The choice of the kink point in the case of the irradiated detectors has an uncertainty due to the not constant value of the capacitance at full depletion. The errors shown in the Tables I and II represent the maximum error of the measurement.

Fig. 6 shows the capacitance per unit area versus reverse bias voltage of an irradiated P-in-N detector. The values of the calculated full depletion voltages for all diodes are shown in Tables I and II. It must be noticed that N-in-P detectors do not reach full depletion before irradiation, and therefore we could not determine the  $V_{FD}$  values. The  $V_{FD}$  theoretical values for P-in-N and N-in-N is 61 V and for N-in-P is 200 V.

### C. Characterization

Fig. 7 shows volume leakage currents versus proton fluence,  $\phi$ , for oxygenated detectors fabricated using the three different technologies. We observe from this figure that all the technologies present almost the same leakage current. Tables III and IV report the parameters  $\alpha$  for a 24 GeV proton fluence and its

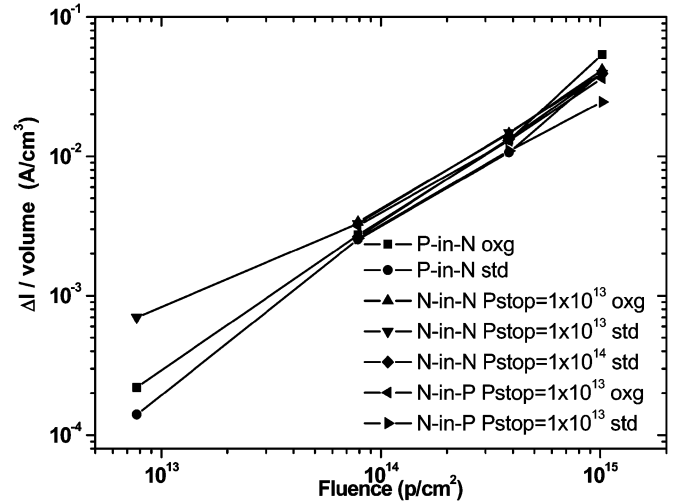


Fig. 7. Fluence dependence of leakage current for detectors fabricated with the three different technologies.

 TABLE III  
 PARAMETER  $\alpha$  VALUES OF P-IN-N AND N-IN-P NORMALIZED TO 20 °C

Technology	P in N		N in P	
	Std	Oxg	Std	Oxg
P-stop	-	-	$10^{13} \text{ cm}^{-2}$	
Substrate	Std	Oxg	Std	Oxg
$\alpha$ ( $\times 10^{-17} \text{ A/cm}$ )	$5.0 \pm 0.4$	$3.8 \pm 0.3$	$4.0 \pm 0.1$	$3.9 \pm 0.0$
$\alpha_{eq}$ ( $\times 10^{-17} \text{ A/cm}$ )	$8.1 \pm 0.7$	$6.1 \pm 0.4$	$6.5 \pm 0.1$	$6.2 \pm 0.0$

 TABLE IV  
 PARAMETER  $\alpha$  VALUES OF N-IN-N AND MEAN OF ALL THE VALUES, NORMALIZED TO 20 °C

Technology	N in N			Mean value of the three technologies
	$10^{14} \text{ cm}^{-2}$	$10^{13} \text{ cm}^{-2}$		
P-stop		Std	Oxg	
Substrate	Std	Std	Oxg	
$\alpha$ ( $\times 10^{-17} \text{ A/cm}$ )	$3.8 \pm 0.1$	$3.6 \pm 0.0$	$2.5 \pm 0.1$	$3.8 \pm 0.3$
$\alpha_{eq}$ ( $\times 10^{-17} \text{ A/cm}$ )	$6.1 \pm 0.1$	$5.7 \pm 0.1$	$4.0 \pm 0.2$	$6.1 \pm 0.5$

equivalent value,  $\alpha_{eq}$ , for a 1-MeV(Si) neutron fluence, calculated for all investigated detectors. Fig. 7 shows the linear fits used to calculate the value of the damage constant,  $\alpha$  [10]. The  $\alpha$  values and errors shown in the tables have been calculated from a linear fit using (1)

$$\frac{\Delta I}{\text{volume}} = \alpha \phi. \quad (1)$$

Currents were normalized to 20 °C according to the following expression [11]:

$$I \approx T^2 \exp\left(\frac{-E_0}{2kT}\right) \quad (2)$$

where  $k$  is the Boltzmann constant, and  $E_0 = 1.12 \text{ eV}$ . The value of  $\alpha$  for the P-in-N in standard silicon is higher than expected, but this sample showed an early breakdown, so it is not reliable. The results are in agreement with the expected values

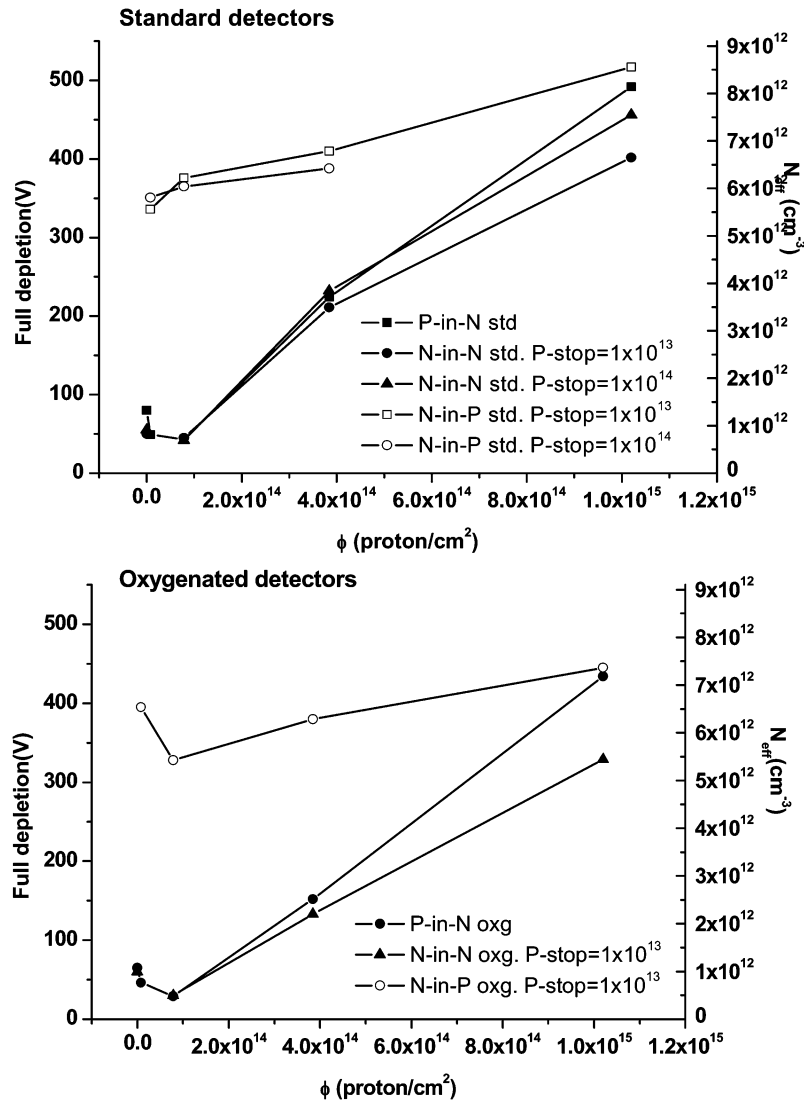


Fig. 8. Full depletion voltage and effective space charge density versus fluences. Top figure shows results for standard silicon while bottom figure shows results for oxygenated silicon detectors.

for an annealing of 4 min at 80 °C [12], except in the case of the N-in-N oxygenated detectors where it is a bit lower.

The effective doping concentrations and full depletion voltages versus fluence are shown in Fig. 8. The values of  $V_{FD}$  at the four fluences are reported for the three different technologies. N-in-N and P-in-N detectors present the expected bulk inversion for irradiation fluences higher than  $10^{13}$  p/cm<sup>2</sup>. As expected, the N-in-P do not show bulk inversion because, at low proton fluences, the change in the effective doping concentration is dominated by donor removal, leading to a decrease in the full depletion voltage. Once the donor removal is exhausted or compensated by acceptors,  $N_{eff}$  reaches a minimum at which the conduction type of the material changes from n-type to p-type. This is the so-called inversion point. For N-type substrates the inversion point is observed at a fluence of  $4 \times 10^{13}$  protons/cm<sup>2</sup>.

Beyond the inversion point, the change in the effective doping concentration and, consequently, in full-depletion voltage, is dominated by deep acceptors generation. The introduction rate of negative space charge beyond the inversion point is modeled

by the  $\beta$  parameter. This has been extracted from linear fits of  $N_{eff}$  versus  $\phi$  well above the inversion point.

Tables V and VI show the value of the parameter  $\beta$  for 24 GeV proton fluence, and the equivalent value for 1-MeV(Si) neutron fluence.  $\beta$  represents the introduction rate of stable defects in irradiated materials and is an important parameter since it controls the operating voltage after the inversion point, leading eventually to breakdown. These values of  $\beta$  have been calculated from the last three points of the curves shown in Fig. 8.

Oxygenation process have a small effect in the beta value for the three technologies. The behavior of P-in-N and N-in-N is similar in terms of  $\beta$ , but N-in-P detectors show a much better performance. Effective doping concentration variation in N-in-P detectors is about half to one third compared to detectors with N-type substrate, as was expected from the absence of type inversion.

From Fig. 8, it seems that N-in-P oxygenated detectors show a bulk inversion at a fluence of  $2.7 \times 10^{14}$  p/cm<sup>2</sup>. But unfortunately, the two first points of this curve, are not reliable due to the presence of a high leakage current. As can be seen from

TABLE V  
PARAMETERS  $\beta$  AND  $\beta_{eq}$  FOR P-IN-N AND N-IN-P DETECTORS

Technology	P in N		N in P	
	Std	Oxg	Std	Oxg
P-stop	---	---	$10^{13} \text{ cm}^{-3}$	
substrate	Std	Oxg	Std	Oxg
$\beta (\times 10^3 \text{ cm}^{-1})$	$7.6 \pm 0.7$	$7.0 \pm 0.2$	$2.5 \pm 0.2$	$2.0 \pm 0.3$
$\beta_{eq} (\times 10^3 \text{ cm}^{-1})$	$12.2 \pm 1.1$	$11.3 \pm 0.3$	$4.0 \pm 0.4$	$3.2 \pm 0.4$

TABLE VI  
PARAMETERS  $\beta$  AND  $\beta_{eq}$  FOR N-IN-N DETECTORS

Technology	N in N		
	$10^{14} \text{ cm}^{-3}$	$10^{13} \text{ cm}^{-3}$	
substrate	Std	Std	Oxg
$\beta (\times 10^3 \text{ cm}^{-1})$	$6.9 \pm 1.1$	$6.0 \pm 0.1$	$5.1 \pm 0.1$
$\beta_{eq} (\times 10^3 \text{ cm}^{-1})$	$11.1 \pm 1.7$	$9.6 \pm 1.5$	$8.3 \pm 0.2$

Fig. 4(b), there is an early breakdown, and the reverse current never reaches a steady value for the two curves of fluence 0 (non irradiated) and  $7 \times 10^{12}$  protons/cm<sup>2</sup>. Because of this, the measurement of  $V_{FD}$  is very difficult or not possible at all. For the two other technologies and for higher radiation doses in N-in-P, we do not have this problem at all, and  $V_{FD}$  is obtained reliably. Nevertheless, this problem does not invalidate the study, the  $\alpha$  and  $\beta$  parameters can be extracted for the rest of the points.

#### IV. CONCLUSIONS AND FUTURE WORK

Detectors based on three different technologies, P-in-N, N-in-N and N-in-P, have been simultaneously fabricated using a full microstrip process. They have been irradiated to fluences up of  $10^{15}$  p/cm<sup>2</sup>, and they work properly.

The value of the parameter  $\alpha$  is similar for the three technologies, as expected, and in agreement with reported values [12].

It has been found that the best value of p-stop implant is  $10^{13} \text{ cm}^{-2}$  for both N-in-N and N-in-P detectors. Detectors with a p-stop of  $10^{14} \text{ cm}^{-2}$  have breakdown voltages lower than the fabricated with a p-stop of  $10^{13} \text{ cm}^{-2}$ , although the leakage currents are comparable.

It has been proved that there is no radiation-induced type inversion in the P-type substrates. The change in effective doping

concentration versus radiation fluence is smaller when compared to N-type substrate technologies. Therefore, the radiation hardness of N-in-P detectors is much higher.

Future works will include charge collection efficiency measurements with alpha and beta particles for the three types of detectors. N-in-P detectors are better in terms of charge collection, as they collect electrons instead of the holes collected in N-type substrates. We expect that charge collection efficiency studies will confirm that the N-in-P technology is the most suitable for ultra-high radiation level environments.

The results obtained for the pad detectors will be compared to those obtained from microstrip detectors fabricated with the same technologies and irradiated with fluences up to  $10^{16}$  protons/cm<sup>2</sup>.

#### ACKNOWLEDGMENT

The authors would like to thank M. Moll and M. Glaser for their support during the irradiations at CERN facilities.

#### REFERENCES

- [1] (1997) ATLAS Inner Detector Tech. Design Rep.. [Online]. Available: <http://cern.ch/atlas>
- [2] G. Casse *et al.*, "Charge collection and charge sharing in heavily irradiated n-side read-out silicon microstrip detectors," *Nucl. Instrum. Meth. A*, vol. 511, pp. 112–117, 2003.
- [3] F. Albiol *et al.*, "Beam test of the ATLAS silicon detector modules," *Nucl. Instrum. Meth. A*, vol. 409, pp. 236–239, 1998.
- [4] G. Casse *et al.*, "Improving the radiation hardness properties of silicon detectors using oxygenated n-type and p-type silicon," *IEEE Trans. Nucl. Sci.*, vol. 47, no. 1, pp. 527–532, Feb. 2000.
- [5] P. P. Allport *et al.*, "Charge collection efficiency studies with irradiated silicon detectors," *Nucl. Instrum. Meth. A*, vol. 501, pp. 146–152, 2003.
- [6] L. F. Fonseca *et al.*, "Silicon wafer oxygenation from SiO<sub>2</sub> layers for radiation hard detectors," *Microelectron. Rel.*, vol. 40, pp. 791–794, 2000.
- [7] Radiation Test Facility at CERN. [Online]. Available: <http://cern.ch/ir-radiation>
- [8] A. Vasilescu and G. Lindstroem. Notes on the fluence normalization based on the NIEL scaling hypothesis. [Online]. Available: ROSE/TN/2000-02 at <http://cern.ch/rd48>
- [9] G. Lindström *et al.*, "Radiation hard silicon detectors developments by the RD48 (ROSE) collaboration," *Nucl. Instrum. Meth. A*, vol. 466, pp. 308–326, 2001.
- [10] (1997) The Rose Collaboration, 1st RD48 Status Rep.. [Online]. Available: CERN/LHCC 97-39, at <http://cern.ch/rd48>
- [11] A. Chilingarov. (2003) Recommendations toward a standardization of the macroscopic parameter measurements. Part I: IV and CV measurements in Si diodes. [Online]. Available: RD50/2003/003 at <http://cern.ch/rd50>
- [12] M. Moll, "Radiation Damage in silicon particle detectors," Ph.D. dissertation, Inst. Experimentalphysik, Univ. Hamburg, Hamburg, Germany, 1999.